

Eclogite-facies metamorphism preserved in tectonic blocks from a lower crustal shear zone, central Transantarctic Mountains, Antarctica

S.M. Peacock^{a,*}, J.W. Goodge^b

^a Department of Geology, Arizona State University, Tempe, AZ 85287-1404, USA

^b Department of Geological Sciences, Southern Methodist University, Dallas, TX 75275-0395, USA

Received 11 October 1994; accepted 13 March 1995

Abstract

In the Geologists and Miller Ranges of the central Transantarctic Mountains, mafic and ultramafic tectonic blocks occur in an Early Cambrian amphibolite- to granulite-facies lower crustal transpressional shear zone. Mafic blocks consist of garnet + clinopyroxene symplectite + hornblende + plagioclase + quartz + ilmenite ± orthopyroxene ± biotite; mineral compositions in these blocks generally reflect equilibration under upper amphibolite to lower granulite facies conditions ($T \sim 700^\circ\text{C}$, $P \sim 8\text{--}12$ kbar). These conditions are the same as those indicated by peak, syn-kinematic assemblages in the enclosing shear zone tectonites. Mineral and textural evidence for an earlier higher-pressure ($P = 12\text{--}25$ kbar) eclogite-facies metamorphism includes: (1) plagioclase reaction rims around anhedral garnet; (2) complex clinopyroxene intergrowths consisting of augite + plagioclase + quartz ± hornblende ± orthopyroxene, interpreted as exsolved Na-rich clinopyroxene (omphacite) and (3) unusual magnesian staurolite [atomic $\text{Mg}/(\text{Mg} + \text{Fe}) = 0.58$] inclusions in pyrope–almandine garnet. We suggest that the relict eclogite-facies metamorphism records an earlier period of crustal thickening that occurred prior to formation of the transpressional shear zone, perhaps as an early stage in Ross orogenesis.

1. Introduction

Eclogitic bands and lenses occur in many migmatitic amphibolite- to granulite-facies gneiss terrains. These eclogites, termed Group B eclogites by Coleman et al. (1965) and medium-temperature eclogites by Carswell (1990), contain mineral assemblages and compositions that reflect metamorphic temperatures of 550–900°C and pressures greater than 12–16 kbar (Carswell, 1990). Medium-temperature eclogites record higher temperatures than eclogite blocks present in blueschist terrains, and they form under lower temper-

atures than eclogite layers in alpine peridotites and eclogite xenoliths in kimberlites (Carswell, 1990).

Eclogites were first described in the Western Gneiss Region of Norway by Eskola (1921). Over the past 70 years, researchers have documented medium-temperature eclogites throughout the Early Paleozoic Caledonian orogenic belt of Scandinavia (e.g., Bryhni et al., 1977; Griffin et al., 1985; Cuthbert and Carswell, 1990) and the Late Paleozoic Variscan orogenic belt of central Europe (see review by O'Brien et al., 1990). Proterozoic medium-temperature eclogites are relatively rare (Carswell and Cuthbert, 1986), but have been documented in the 1.1–1.0 Ga Grenville orogenic belt [Glenelg, northwest Scotland (Sanders et al.,

* Corresponding author.

1984; Sanders, 1989); Llano uplift, Texas (Wilkerson et al., 1988)] and the 1.9–1.8 Ga Nagsugtoqidian orogenic belt in East Greenland (Messiga et al., 1990). In this paper we document the occurrence of latest Neoproterozoic (?) eclogite blocks within a lower-crustal metamorphic complex of the Ross orogenic belt in the central Transantarctic Mountains. The presence of these high-pressure eclogite blocks indicates that at least some basement of the East Antarctic craton involved in Ross orogenesis has a deep-crustal origin.

2. Geologic setting

In the central Transantarctic Mountains in the vicinity of the Nimrod Glacier (Fig. 1), high-grade ductile tectonites of the Miller Range shear zone record deep-crustal left-lateral shear along the Neoproterozoic – Early Paleozoic Antarctic plate margin (Goodge et al., 1993a). Pelitic schist, metacarbonate, amphibolite and quartzofeldspathic gneiss of the Nimrod Group were penetratively deformed under upper amphibolite to lower granulite facies conditions (Goodge et al., 1992); mineral assemblages and geothermobarometry indicate syntectonic metamorphic (M2) pressures ≥ 8 kbar and temperatures $\sim 700^\circ\text{C}$ (Goodge et al., 1992). Peak dynamothermal metamorphism occurred in earliest Paleozoic time, between about 540–520 Ma (Goodge and Dallmeyer, 1992; Goodge et al., 1993b).

Numerous mafic and ultramafic tectonic blocks occur within the ductilely sheared Nimrod Group host rocks, particularly along the boundaries separating pelitic schist from quartzofeldspathic gneiss (Fig. 1B, C). The ellipsoidal to subspherical mafic and ultramafic blocks range in size from 0.5 to 50 m in diameter. Ultramafic blocks are not as common as mafic blocks in the Miller and Geologists Ranges. In some areas, the mafic blocks appear to have once formed a continuous layer that was subjected to boudinage during later deformation (Fig. 2A, B); in other areas, the tectonic blocks occur as isolated blocks of unknown origin (Fig. 2C). Tectonite foliation in the host schists and gneisses wraps around the tectonic blocks (Fig. 2B, C). Foliation within the blocks, where present, is generally discordant to the foliation in the enclosing schists and gneisses. Dilational veins within the blocks containing plagioclase + quartz terminate against the boundary with host gneisses; where asymptotic to the block mar-

gin (Fig. 2D), these veins show a rotational sense of vorticity that is compatible with sense of shear in the enclosing tectonites as determined from asymmetric fabrics (Goodge et al., 1993a). Most mafic tectonic blocks have amphibolitic rinds consisting of hornblende + plagioclase \pm biotite \pm garnet (Fig. 2A, B), whereas the cores of the blocks preserve evidence for an earlier (M1) eclogite-facies metamorphic event that is the principal subject of this paper. These general relations are summarized in Fig. 3.

3. Petrology of mafic blocks

The cores of mafic tectonic blocks contain the mineral assemblage garnet + clinopyroxene symplectite + hornblende + plagioclase + quartz + ilmenite \pm orthopyroxene \pm biotite. Representative microprobe analyses of these minerals are presented in Tables 1–3.

Garnet generally occurs as anhedral grains, 0.25 to 0.5 mm in diameter, surrounded by 25–50 μm rims of plagioclase feldspar (Fig. 4A–D). Quartz and plagioclase occur as very fine-grained inclusions. Garnet compositions in most samples are 55–70 mol % almandine component, 13–22 mol % pyrope, 15–24 mol % grossular, and ~ 2 mol % spessartine (Table 1). Most garnet compositions plot within the Group C eclogite field (Fig. 5) of Coleman et al. (1965) and Mottana (1986), although there is considerable overlap with Mottana's (1986) Group B eclogite field. Garnets ($X_{\text{py}} = 0.13\text{--}0.22$) in the mafic tectonic blocks are significantly richer in magnesium than garnets ($X_{\text{py}} = 0.05\text{--}0.12$, J. Goodge, unpubl. data) in mafic amphibolites from the enclosing tectonites.

Clinopyroxene occurs as optically-continuous grains (0.5–1.0 mm across), intergrown with plagioclase + quartz \pm hornblende \pm orthopyroxene (Fig. 4). Compositionally, the clinopyroxene is augite with 3–6 mol % jadeite (Table 2). We analyzed clinopyroxene intergrowths in one sample using a broad (100 μm diameter) electron beam in order to obtain an average composition for the clinopyroxene intergrowths. An average of nine analyses of different areas yielded a reasonably good pyroxene stoichiometry with 13 mol % jadeite (Table 2).

Green-brown hornblende occurs as anhedral grains < 0.5 mm across. In many samples, secondary green-blue hornblende or actinolite is also present.

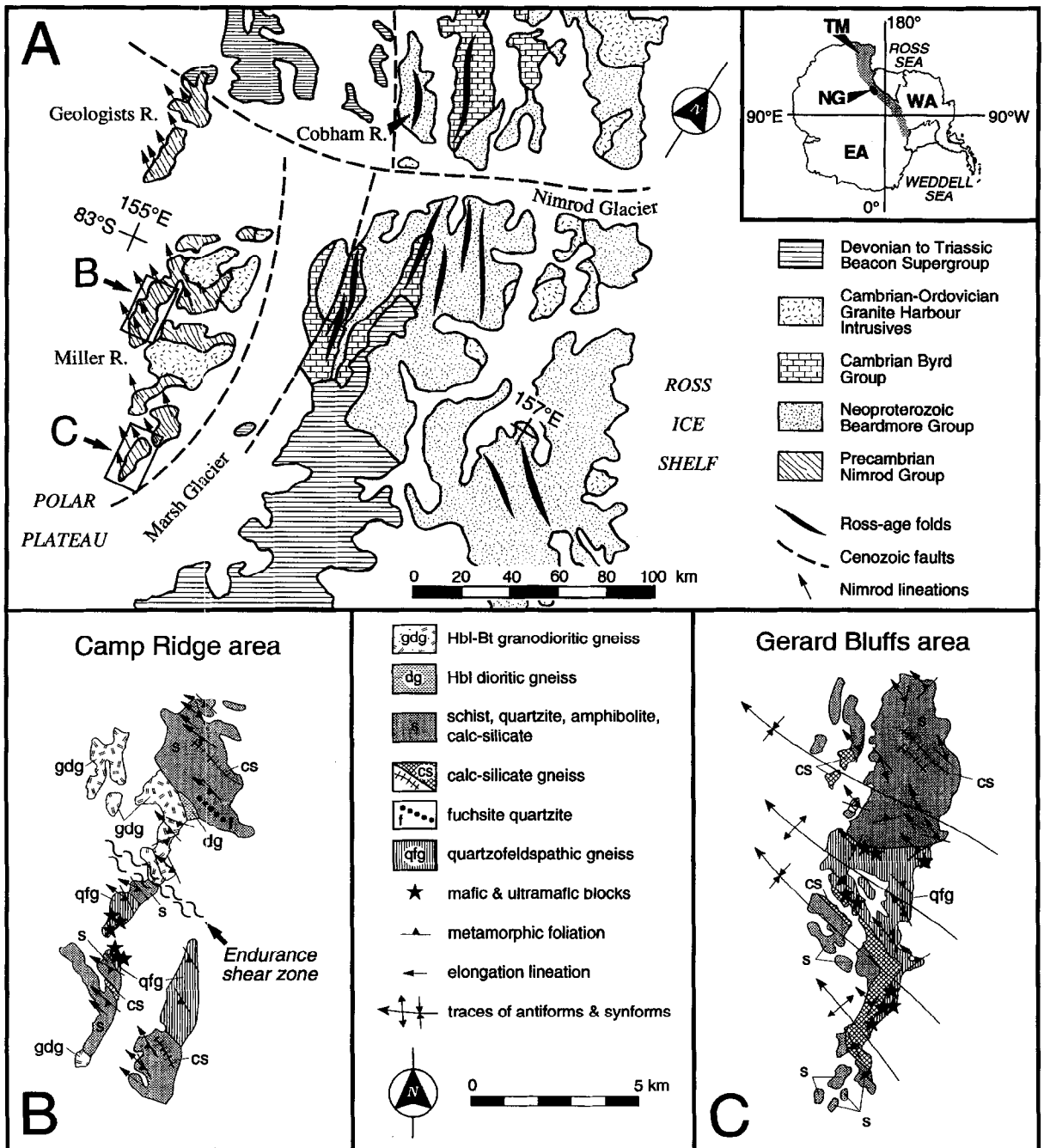


Fig. 1. (A) Generalized geologic map of the central Transantarctic Mountains in the Nimrod Glacier area (from Grindley and Laird, 1969; Goode et al., 1993a). Locations of B and C shown by boxes. Inset shows location in Antarctica. EA, East Antarctica; NG, Nimrod Glacier area; TM, Transantarctic Mountains; WA, West Antarctica. Mafic and ultramafic blocks occur in several areas of the Geologists and Miller ranges, as shown in the examples of B and C. (B) Geologic sketch map of the Camp Ridge area, west-central Miller Range (from Goode et al., 1993a), where numerous mafic blocks containing eclogitic cores occur within quartzofeldspathic schist and gneiss structurally below a continuous schist belt. The blocks lie above the Endurance shear zone, a zone of particularly high shear strain within the larger Miller Range shear zone (Goode et al., 1993a). (C) Geologic sketch map of the Gerard Bluffs area, southern Miller Range (from Goode et al., 1993a). In this area, mafic and ultramafic blocks decorate the contact between quartzofeldspathic gneiss and structurally overlying schist and calc-silicate gneiss. Legend in lower center is for B and C.

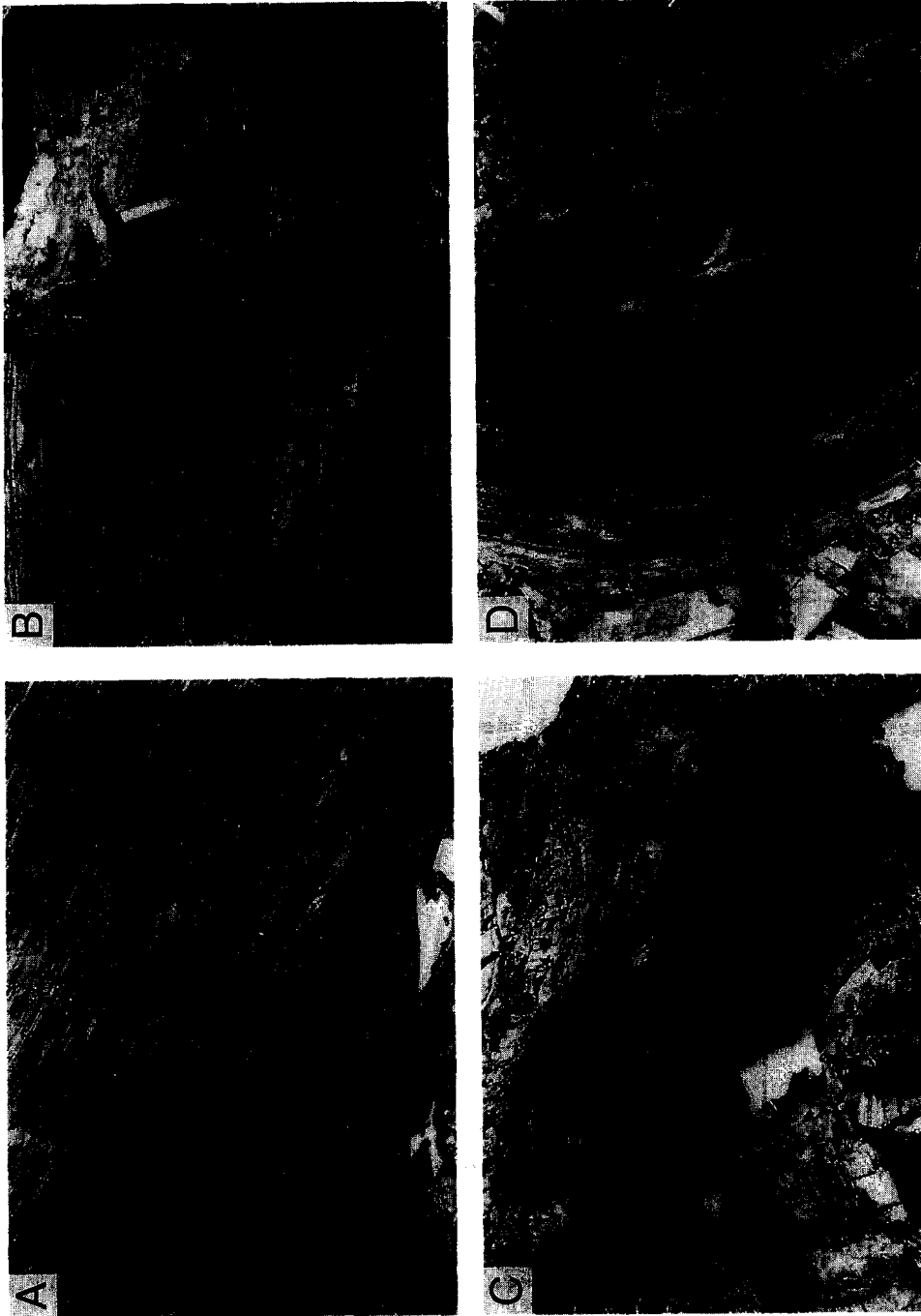


Fig. 2. Photographs showing structural setting of eclogitic blocks within ductile tectonites of the Miller Range shear zone. (A) Train of mafic blocks within layered gneisses exposed in cliff face of Gerard Bluffs area, southern Miller Range. Blocks are several meters in size, and show zonation from dark rim (amphibolite) to lighter core. View shows three blocks in center-right and at least two other blocks in upper left, all within the same layer horizon. (B) Small detached mafic blocks (mostly amphibolite) from the Camp Ridge area of the western Miller Range, showing tails indicative of origin by boudinage. Hammer is 33 cm long. (C) Isolated mafic block wrapped by foliation of enclosing schists, from the Camp Ridge area of the western Miller Range. Block shows dark rim (amphibolite) surrounding dark core of relict eclogite. Hammer is 33 cm long. (D) Margin of block in C (right), showing strong layer attenuation of host schists along contact and curving veins of plagioclase + quartz that are asymptotic to block margin and do not cross into schists. Pen is 14 cm long.

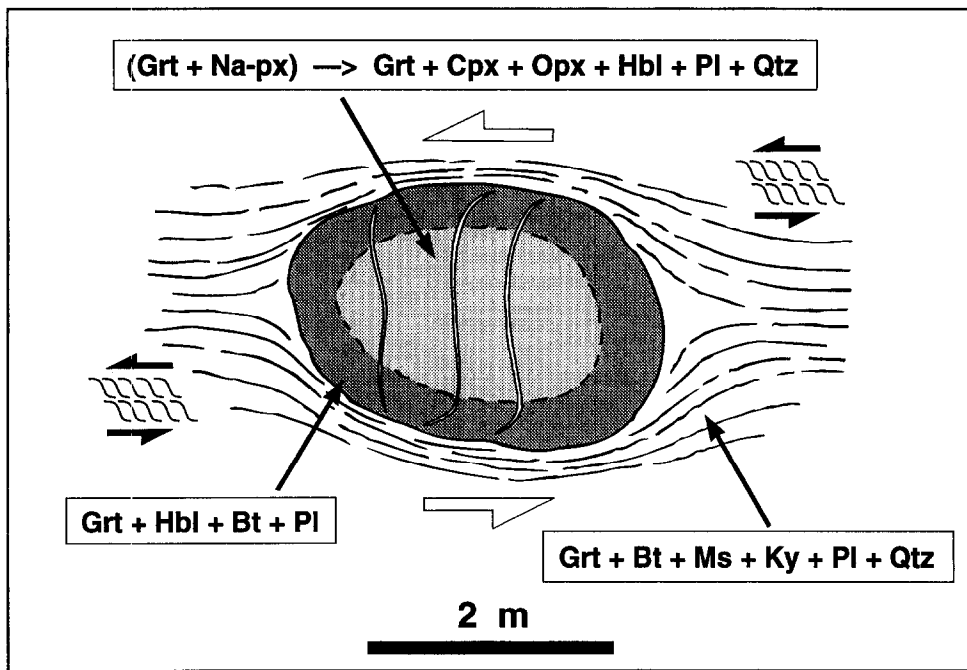


Fig. 3. Sketch showing outcrop and mineralogical characteristics of mafic tectonic blocks. Mafic block cores contain relict eclogite-facies assemblages (light shading), and block rinds contain amphibolite-facies overprint parageneses (dark shading). Pelite tectonites contain *Ky*-bearing assemblages indicative of high-*P* amphibolite-facies deformation. Plagioclase veins cross-cut the blocks, and they display curved forms and tapered ends indicating formation during block rotation. Open arrows show sense of rotation of blocks, and shear sense from asymmetric fabrics in tectonite matrix is indicated.

Plagioclase feldspar occurs as inclusions in clinopyroxene and garnet, and as distinctive rims around anhedral garnet grains. Plagioclase compositions range from An_{25} to An_{40} .

An unusual Mg-rich tectonic block (samples ANT-53G and ANT-53H) from the Camp Ridge area in the Miller Range contains pyrope-rich garnet ($Py_{43-52} Alm_{38-45} Gr_{8-16} Sp_1$) (Table 1, Fig. 5) with inclusions of magnesian staurolite. The core of the block (sample ANT-53G) consists of hornblende + clinopyroxene + garnet; the rim of the block (sample ANT-53H) consists of hornblende + orthopyroxene + garnet + biotite. Fine-grained talc occurs as an alteration of orthopyroxene and clinopyroxene. The interior of a large 7-mm-diameter garnet from the block rim contains a dense cluster of anhedral magnesian staurolite grains up to 0.3 mm across (Fig. 4E, F). The magnesian staurolite exhibits pale orange pleochroism and contains more magnesium than iron [atomic $Mg/(Mg + Fe) = 0.58$] (Table 3). This mineral composition is termed the magnesium analogue of staurolite by the recently

adopted I.M.A. guidelines (IMA No. 92-035, *Can. Mineral.*, 32: 724). Magnesian staurolite inclusions occur in contact with biotite and Ni-arsenide inclusions; the garnet also contains inclusions of quartz and allanite, but these are not observed in contact with magnesian staurolite.

4. Petrology of ultramafic blocks

Several distinct types of ultramafic blocks occur in the Miller and Geologists Ranges, in which primary igneous minerals are variably replaced by hydrous metamorphic minerals.

In the most common type of ultramafic block, relict coarse-grained olivine and orthopyroxene are replaced by the metamorphic assemblage tremolite (or tremolitic hornblende) + chlorite ± talc. For example, in sample ANT-8C from the Geologists Range, olivine (Fo_{88}) + orthopyroxene (En_{87}) have been largely replaced by the assemblage tremolitic horn-

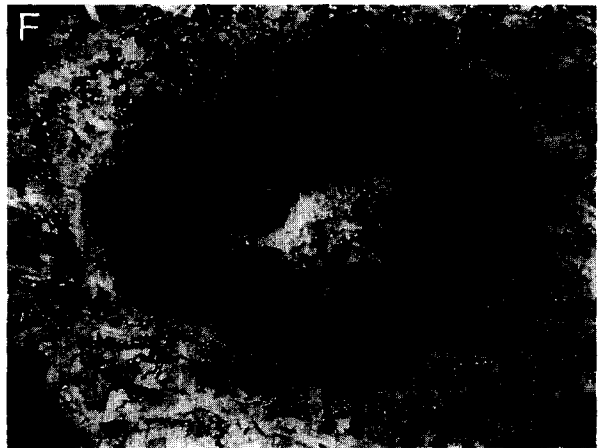
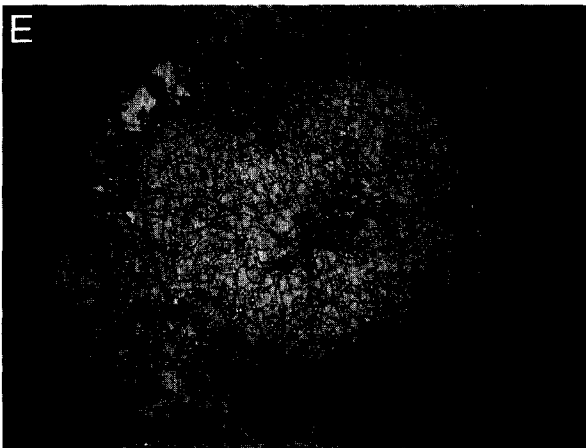
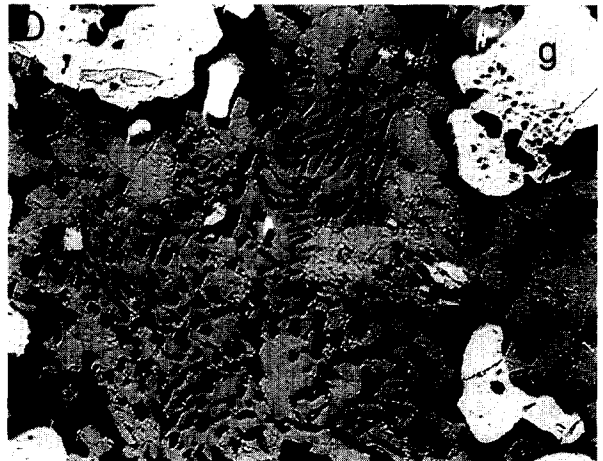
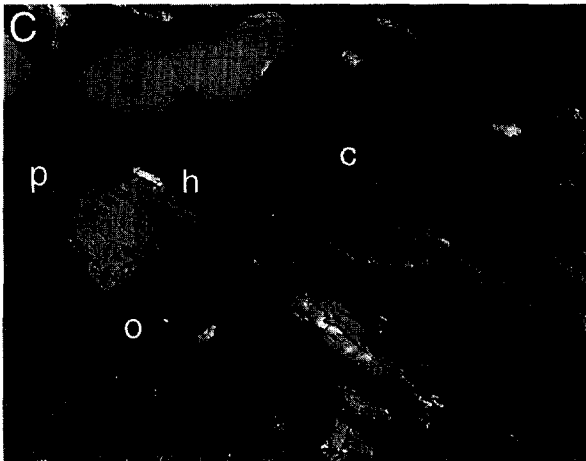
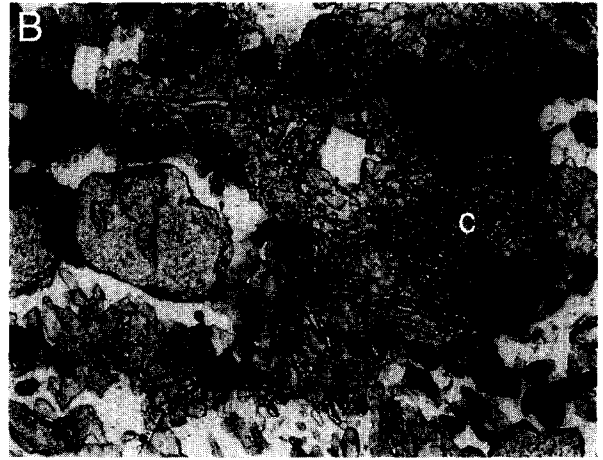
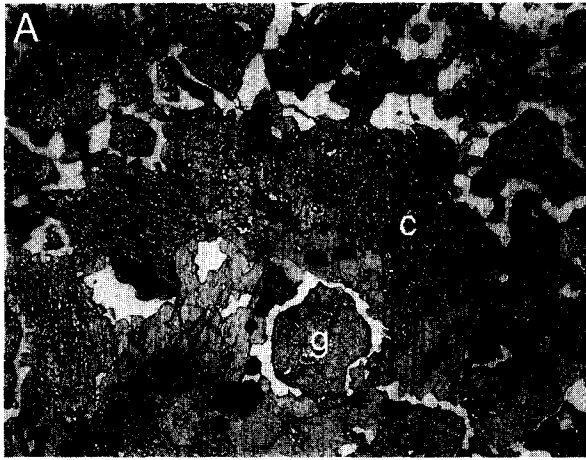


Table 1
Representative electron microprobe analyses of garnet from mafic blocks

Sample <i>n</i>	ANT-53G 3	ANT-53H 9	ANT-53D 3	ANT-54H 9	89-65A 5	90-130A 5	90-130B 7	90-130C 5	90-130D 5
SiO ₂	40.09	40.54	38.86	38.41	38.57	39.04	39.03	38.94	38.15
TiO ₂	0.02	0.02	0.09	0.04	0.16	0.15	0.09	0.05	0.08
Al ₂ O ₃	22.62	23.14	21.84	21.40	21.43	21.70	21.67	21.79	21.06
Cr ₂ O ₃	0.53	0.12	n.a.	n.a.	n.a.	n.a.	n.a.	n.a.	n.a.
FeO ^F	19.38	20.20	26.68	31.09	23.12	22.78	23.52	23.41	27.51
MnO	0.69	0.60	0.82	0.74	0.54	0.48	0.52	0.51	0.58
MgO	11.85	12.88	4.88	3.90	6.83	7.97	6.97	6.80	4.91
CaO	5.61	3.78	7.96	6.02	8.18	7.79	8.52	8.46	7.27
Na ₂ O	0.01	0.00	0.02	0.01	n.a.	n.a.	n.a.	n.a.	n.a.
K ₂ O	0.00	0.01	0.00	0.00	n.a.	n.a.	n.a.	n.a.	n.a.
Total	100.80	101.29	101.15	101.61	98.83	99.91	100.32	99.96	99.57
Si	2.983	2.987	3.003	2.999	3.005	2.996	3.000	3.001	3.006
Ti	0.001	0.001	0.005	0.002	0.009	0.009	0.005	0.003	0.005
Al	1.984	2.010	1.990	1.970	1.969	1.964	1.964	1.980	1.957
Cr	0.023	0.005	n.a.	n.a.	n.a.	n.a.	n.a.	n.a.	n.a.
Fe ²⁺	1.206	1.245	1.725	2.031	1.507	1.462	1.512	1.509	1.813
Mn	0.043	0.037	0.054	0.049	0.036	0.031	0.034	0.033	0.039
Mg	1.314	1.414	0.562	0.454	0.793	0.912	0.798	0.781	0.577
Ca	0.447	0.298	0.659	0.504	0.683	0.641	0.702	0.699	0.614
Na	0.001	0.000	0.003	0.002	n.a.	n.a.	n.a.	n.a.	n.a.
K	0.000	0.001	0.000	0.000	n.a.	n.a.	n.a.	n.a.	n.a.
X(gr)	0.15	0.10	0.22	0.17	0.23	0.21	0.23	0.23	0.20
X(sp)	0.01	0.01	0.02	0.02	0.01	0.01	0.01	0.01	0.01
X(py)	0.44	0.47	0.19	0.15	0.26	0.30	0.26	0.26	0.19
X(alm)	0.40	0.42	0.58	0.67	0.50	0.48	0.50	0.50	0.60

Garnet analyses normalized to 12 oxygens. All iron calculated as ferrous iron. Electron microprobe analyses were obtained at Arizona State University and at Southern Methodist University using natural mineral and synthetic standards.

blende + Mg-chlorite + Cr-bearing magnetite. Relict olivine and orthopyroxene form optically continuous grains up to 5 mm across. Metamorphic amphibole and chlorite grains range from 0.1 to 1.0 mm in size. Locally, very fine-grained ($\sim 1 \mu\text{m}$) talc and serpentine (lizardite) replace orthopyroxene and olivine.

In other ultramafic blocks, large orthopyroxene \pm olivine grains are replaced by coarse-grained anthophyllite + talc + carbonate. Small amounts of very fine-grained serpentine and talc also occur in the anthophyllite-bearing samples.

Fig. 4. (A) Photomicrograph of anhedral garnet (*g*) rimmed by plagioclase (white) and complex clinopyroxene intergrowths (*c*) after omphacitic pyroxene. Plane-polarized light. Long dimension of photomicrograph = 2.3 mm. Sample ANT-54H. (B) Photomicrograph of anhedral garnet (*g*) rimmed by plagioclase (*p*) and complex clinopyroxene intergrowths (*c*) after omphacitic pyroxene. Plane-polarized light. Long dimension of photomicrograph = 0.93 mm. Sample ANT-53D. (C) Backscattered-electron micrograph of exsolution lamellae in clinopyroxene intergrowths consisting of diopsidic clinopyroxene (*c*), hornblende (*h*), orthopyroxene (*o*), plagioclase (dark lamellae), ilmenite, and quartz. Garnet (*g*) rimmed by plagioclase (*p*). Long dimension of micrograph = 0.61 mm. Sample ANT-54H. (D) Backscattered-electron micrograph of clinopyroxene intergrowths consisting primarily of diopside (light gray, smooth texture), hornblende (light gray, pitted texture), and plagioclase (dark grey). Garnet (*g*). Mineral contrast enhanced with z-step proportional to backscattered electron intensity. Long dimension of micrograph = 0.94 mm. Sample ANT-53D. (E) Photomicrograph of large pyrope-rich garnet (*g*) containing abundant magnesian staurolite (*s*) inclusions. Plane-polarized light. Long dimension of photomicrograph = 9.3 mm. Sample ANT-53H. (F) Same as (E) in cross-polarized light.

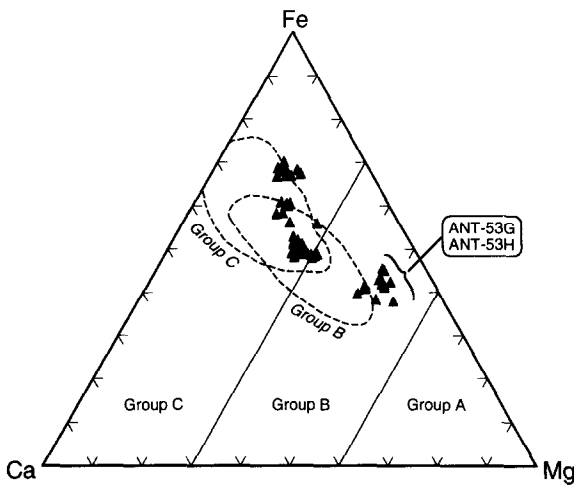


Fig. 5. Fe–Ca–Mg ternary diagram showing composition of garnets in mafic tectonic blocks. Garnet compositions plot within the Group B and C eclogite fields of Coleman et al. (1965) (straight solid lines) and Mottana (1986) (dashed lines). Data points represent electron microprobe analyses of garnets in nine different samples. Cluster of Mg-rich garnet compositions represent two samples (ANT-53G and ANT-53H) from a single eclogitic block. Garnet in ANT-53H contains inclusions of magnesian staurolite (Fig. 4E and F).

The metamorphic mineral assemblages, tremolite + chlorite \pm talc and anthophyllite + talc + carbonate, in ultramafic bulk compositions indicate amphibolite-facies metamorphism (Robinson et al., 1982). The mineral assemblages in the ultramafic blocks are therefore consistent with the upper-amphibolite facies M2 metamorphic assemblages in the host gneisses and schists, indicating that the ultramafic blocks probably were metamorphosed along with the enclosing gneisses during M2. Because primary anhydrous minerals are preserved locally, the metamorphism of the ultramafic rocks principally involved hydration reactions. We interpret the existing hydrous assemblages as the product of simple hydration during high-grade M2, during which time abundant devolatilization reactions in the volumetrically-dominant gneisses and schists were releasing aqueous fluid. The very fine-grained serpentine + talc alteration probably records relatively low-temperature, post-M2 retrograde mineral growth. The ultramafic blocks examined in this study contain no record of the earlier, eclogite-facies metamorphism observed in the mafic blocks, and their petrologic significance is not discussed further here.

5. Constraints on M1 pressure and temperature

Among the different block types described above, the mafic blocks are most helpful in documenting the complete petrogenetic history of the Nimrod Group, and they are the focus of our discussion below. The ultramafic blocks, while important to note, do not constrain the conditions of early metamorphism. Several lines of textural and mineralogical evidence indicate that the mafic blocks were metamorphosed in the eclogite facies prior to reequilibration at lower pressure in the upper amphibolite to lower granulite facies.

(1) The distinctive plagioclase rims around garnet is a characteristic texture of eclogite-facies rocks that have reequilibrated under lower pressure, crustal conditions (e.g., Messiga et al., 1990). In the tectonic blocks, plagioclase commonly separates anhedral garnet grains from clinopyroxene intergrowths (Fig. 4A–D). Given that plagioclase is not stable within the eclogite facies, this texture indicates that early coexisting garnet and clinopyroxene reacted to form plagioclase as a result of decompression.

(2) The complex clinopyroxene intergrowths appear to have formed by exsolution of a more Na-rich pyroxene. Na-rich pyroxene (omphacite) is stable in the eclogite facies. Broad-beam electron microprobe analysis of the clinopyroxene intergrowths yielded a more Na-rich composition, but true omphacite compositions were not recovered. We suggest that Na migrated beyond the original omphacitic clinopyroxene grain boundaries, as would be required in order to produce the observed intermediate-composition plagioclase rims around garnet.

(3) The unusual magnesian staurolite inclusions present in a pyrope-rich garnet from the Miller Range probably formed under eclogite-facies conditions. Ferroan staurolite, a common mineral in amphibolite-facies pelites, is stable at $P < 15$ kbar and $T \sim 500$ – 700°C in the K_2O – FeO – Al_2O_3 – SiO_2 – H_2O system (Spear and Cheney, 1989) (Fig. 6). Magnesian staurolite is an exceptionally rare mineral and magnesium-rich staurolite has only been reported from a few localities (Table 4). Among these are relict staurolite inclusions in tourmaline from a mafic lithology in the Lanterman metamorphic complex of northern Victoria Land (Grew and Sandiford, 1984), which records a metamorphic P – T history that is similar to that of the Nimrod Group M2. According to experiments of

Table 2
Representative electron microprobe analyses of amphiboles and pyroxenes from mafic blocks

Sample	Amphibole				Clinopyroxene				Orthopyroxene	
	ANT-53G	ANT-53H	ANT-53D	ANT-54H	ANT-53G	ANT-53D	ANT-54H	ANT-54H	ANT-53H	ANT-54H
<i>n</i>	3	3	3	4	4	3	7	9 ^a	4	7
SiO ₂	51.48	51.22	44.72	45.92	54.79	52.88	52.46	51.79	55.10	50.93
TiO ₂	0.41	0.18	1.60	1.28	0.02	0.17	0.06	0.15	0.00	0.03
Al ₂ O ₃	6.98	7.80	11.37	9.80	1.57	1.98	1.11	5.50	1.16	0.52
Cr ₂ O ₃	0.35	0.18	n.a.	n.a.	0.48	n.a.	n.a.	0.02	n.a.	n.a.
FeO ^F	5.67	8.70	14.49	17.06	3.16	9.20	12.38	12.74	13.83	32.65
MnO	0.07	0.10	0.03	0.09	0.03	0.13	0.11	0.08	0.15	0.26
MgO	18.92	19.89	11.61	10.72	15.68	12.76	11.55	9.84	29.15	15.17
CaO	11.24	8.26	11.34	10.79	23.16	21.63	21.71	16.39	0.17	0.62
Na ₂ O	1.53	0.96	1.48	1.70	1.12	0.47	0.44	1.72	0.01	0.00
K ₂ O	0.25	0.13	0.88	0.39	0.00	0.03	0.00	0.09	0.01	0.00
Total	96.90	97.41	97.51	97.75	100.01	99.25	99.82	98.32	99.58	100.18
Si	7.262	7.202	6.612	6.820	1.994	1.983	1.988	1.964	1.972	1.989
Al (iv)	0.738	0.798	1.388	1.180	0.006	0.017	0.012	0.036	0.028	0.011
Al (vi)	0.423	0.495	0.595	0.536	0.061	0.071	0.038	0.210	0.021	0.013
Cr	0.029	0.015	n.a.	n.a.	0.010	n.a.	n.a.	0.000	n.a.	n.a.
Ti	0.044	0.019	0.178	0.143	0.001	0.005	0.002	0.004	0.000	0.001
Fe ²⁺	0.669	1.023	1.793	2.119	0.096	0.289	0.392	0.404	0.414	1.067
Mn	0.008	0.012	0.003	0.011	0.001	0.004	0.004	0.003	0.005	0.009
Mg	3.978	4.168	2.557	2.373	0.850	0.713	0.652	0.556	1.555	0.883
Ca	1.699	1.244	1.797	1.717	0.903	0.869	0.881	0.666	0.007	0.026
Na	0.418	0.262	0.425	0.489	0.079	0.034	0.032	0.126	0.001	0.000
K	0.045	0.023	0.166	0.074	0.000	0.001	0.000	0.004	0.000	0.000
Σ Cations	15.313	15.261	15.514	15.462	4.001	3.986	4.001	3.973	4.003	3.999
Mg/(Mg + Fe)	0.86	0.80	0.59	0.53	0.90	0.71	0.62	0.58	0.79	0.45

^aBroad beam electron microprobe analysis of clinopyroxene intergrowths. Amphibole analyses normalized to 23 oxygen equivalents; pyroxene analyses normalized to 6 oxygens.

Schreyer (1988), pure Mg-staurolite is stable in the MgO–Al₂O₃–SiO₂–H₂O system at $P > 14$ kbar and $T > 710$ – 760°C (Fig. 6). Significantly, magnesian staurolite (Mg# = 53–57) was synthesized experimentally by Hellman and Green (1979) in two mafic compositions at $P = 24$ – 26 kbar and $T = 740$ – 760°C ; their synthesized staurolite has a composition very close to the magnesian staurolite (Mg# = 58) reported in this study. Both of the experimental studies indicate that the staurolite in this mafic block formed at pressures well into the range of eclogite-facies metamorphism.

The pyrope-rich garnets, complex clinopyroxene intergrowths and the magnesian staurolite provide strong relict evidence for an early eclogite-facies metamorphic event. Later upper amphibolite–lower gran-

ulite facies metamorphism resulted in extensive reequilibration of mineral assemblages and mineral compositions. Given the extensive upper amphibolite–lower granulite facies reequilibration, it is not possible to quantitatively constrain the metamorphic pressures and temperatures of the earlier eclogite-facies metamorphism. Based on the observations discussed above and the broad P – T constraints depicted in Fig. 6, we suggest that eclogite-facies metamorphism took place at pressures greater than 12–16 kbar and temperatures between 600 and 900°C, corresponding to the medium-temperature eclogite facies of Carswell (1990). The presence of magnesian staurolite in at least one block suggests metamorphic pressures may have been significantly higher.

6. Inferred tectonic setting

The concentration of eclogitic and ultramafic blocks in the vicinity of a mapped boundary between quartzofeldspathic gneisses and other heterogeneous schists, indicates that the eclogites and ultramafic rocks may mark the location of a fundamental tectonic boundary within the Nimrod Group, as first suggested by Grindley (1972). However, detailed field study showed that this lithologic boundary is not characterized by any clear structural discontinuities (Goodge et al., 1992). Because the Nimrod Group rocks in these areas and elsewhere in the Miller and Geologists Ranges consti-

Table 3
Representative electron microprobe analyses of minerals from mafic blocks

Sample	Staurolite			Biotite			Talc			Plagioclase	
	ANT-53H	ANT-53H	ANT-53G	53D	54H	53D	54H	53D	54H	53D	54H
<i>n</i>	3	3	1	3	8						
SiO ₂	28.04	39.34	58.42	SiO ₂	59.99	62.20					
TiO ₂	0.45	0.91	0.03	Al ₂ O ₃	26.14	24.66					
Al ₂ O ₃	56.41	18.17	1.13	CaO	7.24	5.91					
Cr ₂ O ₃	0.13	0.11	0.14	Na ₂ O	7.07	8.08					
FeO ^T	7.48	5.61	6.31	K ₂ O	0.32	0.16					
MnO	0.02	0.07	0.04	Total	100.76	101.01					
MgO	5.89	21.47	26.48	Si	2.651	2.730					
CaO	0.00	0.00	0.16	Al	1.362	1.276					
Na ₂ O	0.00	0.09	0.25	Ca	0.343	0.278					
K ₂ O	0.00	8.82	0.02	Na	0.606	0.688					
Total	98.41	94.59	92.98	K	0.018	0.009					
Si	7.510	2.795	3.913	Total	4.980	4.981					
Al (iv)	0.490	1.205	0.087	X (ab)	0.63	0.70					
Al (vi)	17.324	0.317	0.002	X (an)	0.36	0.29					
Cr	0.021	0.005	0.006	X (or)	0.02	0.01					
Ti	0.091	0.049	0.002								
Fe ²⁺	1.676	0.333	0.354								
Mn	0.005	0.004	0.002								
Mg	2.351	2.274	2.643								
Ca	0.000	0.000	0.011								
Na	0.000	0.012	0.032								
K	0.000	0.800	0.002								
Σ Cations	29.468	7.794	7.054								
Mg											
(Mg + Fe)	0.58	0.87	0.88								

Staurolite analysis normalized to 23 oxygen equivalents; biotite and talc analyses normalized to 11 oxygen equivalents; plagioclase feldspar analyses normalized to 8 oxygens.

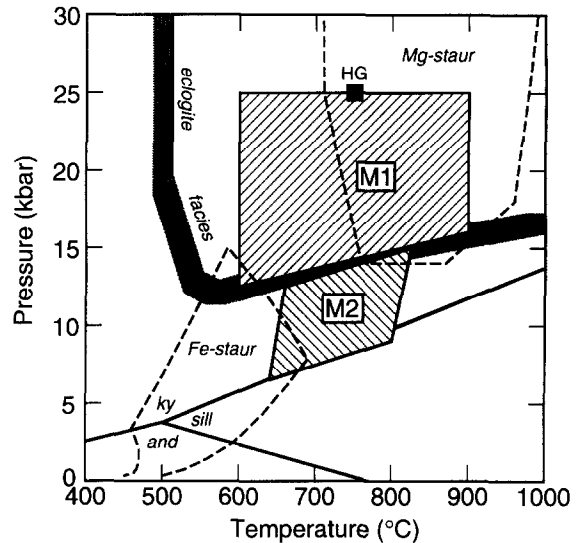


Fig. 6. Pressure-temperature diagram showing constraints on early eclogite (*M1*) metamorphism preserved in mafic blocks and syntectonic upper amphibolite-lower granulite (*M2*) metamorphism of host schists and gneisses determined from mineral assemblages and geothermobarometry (Goodge et al., 1992). *Fe-staur* = maximum stability field of Fe-staurolite in the KFLASH system based on thermodynamic calculations (Spear and Cheney, 1989). *Mg-staur* = maximum stability field of Mg-staurolite in the MASH system based on experiments (Schreyer, 1988). *HG* = experimental run conditions of Hellman and Green (1979) in which magnesian staurolite (Mg# 53–57) was synthesized in two mafic compositions. Shaded band shows boundaries of eclogite facies from Peacock (1993) based on facies diagrams presented by Turner (1981), Liou et al. (1985), Oh et al. (1988), and Evans (1990). *Al₂SiO₅* triple point after Holdaway (1971); *and*, andalusite; *ky*, kyanite; *sill*, sillimanite.

tute a wide ductile shear zone, it is impossible to determine the original geologic setting of the block protoliths. The boudinaged form of the blocks within the ductile matrix is primarily the result of a rheological contrast between different rock types during shear at high strain rates (Goodge et al., 1993a), and it does not constitute evidence for initial structural entrainment. Thus, the present structural setting of these blocks has no bearing on their origin.

The age of eclogite-facies metamorphism within the blocks is poorly constrained. Ductile deformation of the host tectonites occurred between about 540–520 Ma (Goodge et al., 1993b), and this is inferred to be the time when the blocks were tectonically fragmented and displaced within the Miller Range shear zone and when their amphibolitic rinds formed. Eclogite-facies

Table 4
Occurrences of Mg-rich staurolite

Locality	Petrology	Mg/Fe + Mg	Reference
Limpopo Belt, Southern Africa	Inclusions in pyrope–almandine garnet in sappharine–garnet–gedrite–spinel–corundum–phlogopite rock	0.49	Schreyer et al. (1984)
Victoria Land, Antarctica	Inclusions in tourmaline in talc–phlogopite–chlorite–albite schist	0.40–0.42	Grew and Sandiford (1984)
Fiordland, New Zealand	Inclusions in hornblende and garnet in a partially metamorphosed hornblende olivine gabbro-norite	0.43–0.46 and 0.55–0.56	Ward (1984)
South Vohibory, Madagascar	In a corundum–garnet–sappharine anorthosite vein	0.52	Nicollet (1986)
Jiangsu province, East China	Secondary pseudomorphs in garnet–corundum rocks and eclogite	0.68–0.72	Enami and Zang (1988)
Miller Range, Antarctica	Inclusions in pyrope–almandine garnet in retrogressed eclogite	0.58	This study

metamorphism must therefore pre-date ductile deformation within the shear zone (i.e., > 540 Ma), but the older age limit is unconstrained.

In the context of these structural and age relations, there are two fundamentally different tectonic interpretations of eclogite blocks enclosed in amphibolite- or granulite-facies gneisses (e.g., Cuthbert and Carswell, 1990): (1) eclogites and enclosing gneisses are metamorphosed together in the eclogite facies (the *in situ* eclogite model), but the mineralogy of the host gneisses is transformed by later retrogression under lower pressure conditions and (2) eclogites form at high (mantle) pressures and are tectonically emplaced into lower-pressure crustal gneisses (the *foreign* eclogite model). The two different models have been hotly debated for eclogites in the Scandinavian Caledonides, but recent recognition of relict eclogite-facies mineral assemblages within the host gneisses provides strong support for the *in situ* model (e.g., Cuthbert and Carswell, 1990). In Nimrod Group rocks of the central Transantarctic Mountains, we have not observed relict eclogite-facies mineral assemblages in the enclosing schists and gneisses. Thus, we can not distinguish between the two models on this basis.

In an *in situ* model, Nimrod Group eclogites represent metamorphic conditions achieved in the lower part of thick (40–90 km) continental crust that may have formed by continent collision. All lithologies, including the host schists and gneisses, were subjected to eclogite-facies metamorphism (M1) at pressures of

12–25 kbar and temperatures of 600–900°C. Denudation after eclogite-facies metamorphism resulted in decompression of the metamorphic terrain to depths of 25–40 km, corresponding to pressures of 8–12 kbar. Penetrative L–S tectonite fabrics subsequently formed during ductile deformation under upper amphibolite to lower granulite facies conditions (M2). Mineral assemblages and mineral compositions in all lithologies, except for rare mafic blocks, completely reequilibrated during the lower pressure, upper amphibolite to lower granulite facies metamorphism. Pervasive reequilibration would be enhanced by the penetrative ductile deformation that affected all lithologies. Mafic blocks did not completely reequilibrate during M2, probably because of their relative resistance to deformation and low permeability. The principal mineralogical response of the mafic eclogite blocks to the lower pressure M2 conditions was the formation of clinopyroxene symplectites and plagioclase coronae around garnet.

In a *foreign* eclogite model, Nimrod Group eclogites formed at high pressures, perhaps at the base of existing continental crust. The eclogites were then tectonically interleaved with lower-pressure metasedimentary and meta-igneous crustal rocks by some sort of suturing or collisional process during M2. The decompression experienced by the eclogitic rocks during such a tectonic event would lead to similar textural and mineralogical changes consistent with amphibolite-facies retrogression. The distribution and size of the eclogite

blocks within the host schists and gneisses presents a structurally complex emplacement problem, similar to the problem associated with explaining low-temperature, high-pressure eclogite blocks in lower-pressure accretionary prism melanges. Perhaps the Antarctic eclogites and their host rocks represent a former Franciscan-type melange that was subsequently metamorphosed under upper amphibolite to lower granulite facies conditions? Such an interpretation might also be extended to a similar occurrence of ultramafic and mafic tectonic blocks along the eastern margin of the Lanterman metamorphic complex in northern Victoria Land, as alluded to by Grew et al. (1984) and Kleinschmidt et al. (1987).

We stress that our data do not permit us to distinguish between the two eclogite models, but we prefer an in situ eclogite model in which all lithologies were first subjected to a pervasive, eclogite-facies M1 metamorphism. Implicit in this preferred interpretation is that M1 conditions are the consequence of thickening associated with collision of continental or quasi-continental crust, and that at least the ultramafic blocks represent fragments of upper mantle material from the overriding plate that were entrained within the collision zone at great depth prior to M2. Eclogite-facies conditions could have been attained by all rocks during the early highest-pressure segment of a clockwise P - T path that culminated in the peak M2 conditions shown in Fig. 6. In this model, formation of the eclogites may represent an early stage in the collision leading to M2 crustal shear, and not an entirely separate event.

7. Conclusions

In the central Transantarctic Mountains, a cryptic Neoproterozoic (?) eclogite-facies metamorphism (M1) is preserved in mafic tectonic blocks within upper amphibolite–lower granulite facies (M2) schists and gneisses. Evidence for eclogite-facies metamorphism includes plagioclase coronae around garnet, clinopyroxene symplectites formed from more Na-rich clinopyroxene and magnesian staurolite inclusions in pyrope–almandine garnet. Metamorphic conditions for the eclogite event are loosely constrained to temperatures between 600 and 900°C and pressures between 12 and 25 kbar. We prefer a model in which all lithologies were subjected to eclogite-facies metamorphism

during a crustal thickening event, followed by extensive reequilibration under lower pressure (8–12 kbar) conditions that resulted in the pervasive development of transitional amphibolite–granulite facies mineral assemblages and compositions.

Acknowledgements

This study was supported in part by the U.S. National Science Foundation (OPP-8816807). The Arizona State University electron microprobe used in this study was purchased with the aid of NSF grant EAR-8408163. We thank E. Grew and A. Mottana for constructive manuscript reviews.

References

- Bryhni, I., Krogh, E. and Griffin, W.L., 1977. Crustal derivation of Norwegian eclogites: a review. *Neues Jahrb. Mineral. Abh.*, 130: 49–68.
- Carswell, D.A. and Cuthbert, S.J., 1986. Eclogite facies metamorphism in the lower continental crust. In: J.B. Dawson, D.A. Carswell, J. Hall and K.H. Wedepohl (Editors), *The Nature of the Lower Continental Crust*. Geol. Soc. Spec. Publ., 24: 193–209.
- Carswell, D.A., 1990. Eclogites and the eclogite facies: definitions and classifications. In: D.A. Carswell (Editor), *Eclogite Facies Rocks*. Chapman and Hall, New York, pp. 1–13.
- Coleman, R.G., Lee, D.E., Beatty, L.B. and Brannock, W.W., 1965. Eclogites and eclogites: Their differences and similarities. *Geol. Soc. Am. Bull.*, 76: 483–508.
- Cuthbert, S.J. and Carswell, D.A., 1990. Formation and exhumation of medium-temperature eclogites in the Scandinavian Caledonides. In: D.A. Carswell (Editor), *Eclogite Facies Rocks*. Chapman and Hall, New York, pp. 180–203.
- Enami, M. and Zang, Q., 1988. Magnesian staurolite in garnet–corundum rocks and eclogite from the Donghai district, Jiangsu province, east China. *Am. Mineral.*, 73: 48–56.
- Eskola, P., 1921. On the eclogites of Norway. *Skr. Vidensk. Selsk. Christiania, Mat.-Natv. KII*, 8: 1–118.
- Evans, B.W., 1990. Phase relations of epidote blueschists. *Lithos*, 25: 2–23.
- Goodge, J.W. and Dallmeyer, R.D., 1992. $^{40}\text{Ar}/^{39}\text{Ar}$ mineral age constraints on the Paleozoic tectonothermal evolution of high-grade basement rocks within the Ross Orogen, Central Transantarctic Mountains. *J. Geol.*, 100: 91–106.
- Goodge, J.W., Hansen, V.L. and Peacock, S.M., 1992. Multiple petrotectonic events in high-grade metamorphic rocks of the Nimrod Group, central Transantarctic Mountains, Antarctica. In: Y. Yoshida et al. (Editors), *Recent Progress on Antarctic Earth Science*. Terra Scientific Publishing Company (TERRAPUB), Tokyo, pp. 203–209.

- Goodge, J.W., Hansen, V.L., Peacock, S.M., Smith, B.K. and Walker, N.W., 1993a. Kinematic evolution of the Miller Range Shear Zone, central Transantarctic Mountains, Antarctica, and implications for Neoproterozoic to Early Paleozoic tectonics of the East Antarctic Margin of Gondwana. *Tectonics*, 12: 1460–1478.
- Goodge, J.W., Walker, N.W., and Hansen, V.L., 1993b. Neoproterozoic–Cambrian basement-involved orogenesis within the Antarctic margin of Gondwana. *Geology*, 21: 37–40.
- Grew, E.S. and Sandiford, M., 1984. A staurolite–talc assemblage in tourmaline–phlogopite–chlorite schist from northern Victoria Land, Antarctica, and its petrologic significance. *Contrib. Mineral. Petrol.*, 87: 337–350.
- Grew, E.S., Kleinschmidt, G. and Schubert, W., 1984. Contrasting metamorphic belts in North Victoria Land, Antarctica. *Geol. Jahrb.*, B60: 253–264.
- Griffin, W.L., Austrheim, H., Brastad, K., Bryhni, I., Krill, A.G., Krogh, E.J., Mork, M.B.E., Qvale, H. and Torudbakken, B., 1985. High-pressure metamorphism in the Scandinavian Caledonides. In: D.G. Gee and B.A. Sturt (Editors), *The Caledonide Orogen — Scandinavia and Related Areas*. Wiley, New York, pp. 783–801.
- Grindley, G.W., 1972. Polyphase deformation of the Precambrian Nimrod Group, central Transantarctic Mountains. In: R.J. Adie (Editor), *Antarctic Geology and Geophysics*. Universitetsforlaget, Oslo, pp. 313–318.
- Grindley, G.W. and Laird, M.G., 1969. Geology of the Shackleton Coast, Antarctica (Sheet 15). In: V.C. Bushnell and C. Craddock (Editors), *Geologic Maps of Antarctica, Antarctic Map Folio Series, Folio 12*. Am. Geogr. Soc., New York.
- Hellman, P.L. and Green, T.H., 1979. The high pressure experimental crystallization of staurolite in hydrous mafic compositions. *Contrib. Mineral. Petrol.*, 68: 369–372.
- Holdaway, M.J., 1971. Stability of andalusite and the aluminum silicate phase diagram. *Am. J. Sci.*, 271: 97–131.
- Kleinschmidt, G., Schubert, W., Olesch, M. and Rettmann, E.S., 1987. Ultramafic rocks of the Lanterman Range in north Victoria Land, Antarctica: Petrology, geochemistry, and geodynamic implications. *Geol. Jahrb.*, B66: 231–273.
- Liou, J.G., Maruyama, S. and Cho, M., 1985. Phase equilibria and mineral parageneses of metabasites in low-grade metamorphism. *Mineral. Mag.*, 49: 321–333.
- Messiga, B., Tribuzio, R. and Vannucci, R., 1990. Mafic and ultramafic pods with eclogitic relics from the proterozoic Nagssugtoqidian mobile belt of East Greenland. *Lithos*, 25: 101–118.
- Mottana, A., 1986. Crystal-chemical evaluation of garnet and omphacite microprobe analysis: its bearing on the classification of eclogites. *Lithos*, 19: 171–186.
- Nicollet, C., 1986. Saphirine et staurolite riche en magnésium et chrome dans les amphibolites et anorthosites à corindon du Vohibory Sud, Madagascar. *Bull. Minéral.*, 109: 599–612.
- O'Brien, P.J., Carswell, D.A. and Gebauer, D., 1990. Eclogite formation and distribution in the European Variscides. In: D.A. Carswell (Editor), *Eclogite Facies Rocks*. Chapman and Hall, New York, pp. 204–224.
- Oh, C.W., Liou, J.G. and Krogh, E.J., 1988. A petrogenetic grid for the eclogite and related facies at high pressure metamorphism. *Geol. Soc. Am. Abstr. Prog.*, 20: A344.
- Peacock, S.M., 1993. The importance of blueschist → eclogite dehydration reactions in subducting oceanic crust. *Geol. Soc. Am. Bull.*, 105: 684–694.
- Robinson, P., Spear, F.S., Schumacher, J.C., Laird, J., Klein, C., Evans, B.W., and Doolan, B.L., 1982. Phase relations of metamorphic amphiboles: Natural occurrence and theory. In: D.R. Veblen and P.H. Ribbe (Editors), *Amphiboles: Petrology and Experimental Phase Relations*. Mineral. Soc. Am., Washington, D.C., pp. 1–227.
- Sanders, I.S., 1989. Phase relations and P–T conditions for eclogite-facies rocks at Glenelg, north-west Scotland. In: J.S. Daly, R.A. Cliff and B.W.D. Yardley (Editors), *Evolution of Mountain Belts*. *Geol. Soc. Spec. Publ.*, 43: 513–517.
- Sanders, I.S., van Calsteren, P.W.C. and Hawkesworth, C.J., 1984. A Grenville Sm–Nd age for the Glenelg eclogite in north-west Scotland. *Nature*, 312: 439–440.
- Schreyer, W., 1988. Experimental studies on metamorphism of crustal rocks under mantle pressures. *Mineral. Mag.*, 52: 1–26.
- Schreyer, W., Horrocks, P.C. and Abraham, K., 1984. High-magnesium staurolite in a sapphirine–garnet rock from the Limpopo Belt, Southern Africa. *Contrib. Mineral. Petrol.*, 86: 200–207.
- Spear, F.S. and Cheney, J.T., 1989. A petrogenetic grid for pelitic schists in the system $\text{SiO}_2\text{–Al}_2\text{O}_3\text{–FeO–MgO–K}_2\text{O–H}_2\text{O}$. *Contrib. Mineral. Petrol.*, 101: 149–164.
- Turner, F.J., 1981. *Metamorphic Petrology: Mineralogical, Field, and Tectonic Aspects*. McGraw-Hill, New York, 524 pp.
- Ward, C.M., 1984. Magnesium staurolite and green chromian staurolite from Fiordland, New Zealand. *Am. Mineral.*, 69: 531–540.
- Wilkerson, A., Carlson, W.D. and Smith, D., 1988. High-pressure metamorphism during the Llano orogeny inferred from Proterozoic eclogite remnants. *Geology*, 16: 391–394.